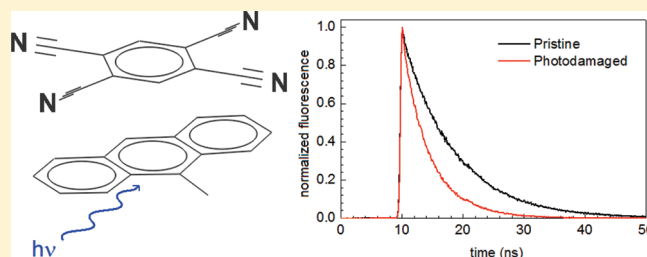


The Effects of Photochemical and Mechanical Damage on the Excited State Dynamics of Charge-Transfer Molecular Crystals Composed of Tetracyanobenzene and Aromatic Donor Molecules

Robert J. Dillon and Christopher J. Bardeen*

Department of Chemistry, University of California, 501 Big Springs Road, Riverside, California 92521, United States

ABSTRACT: Charge-transfer molecular crystals are structurally well-defined systems whose electron transfer dynamics can be studied using time-resolved spectroscopy. In this paper, five 1:1 complexes, consisting of 1,2,4,5-tetracyanobenzene as the electron acceptor and durene, 9-methylanthracene, naphthalene, phenanthrene, and pyrene as electron donors, are studied using time-resolved fluorescence and transient absorption in the diffuse reflectance geometry. Two different sample morphologies were studied: single crystals and powders prepared by pulverizing the crystals and diluting them with barium sulfate microparticles. Fluorescence lifetime and transient absorption measurements performed on the crystals and the powders yielded different results. The crystals typically exhibited long-lived monoexponential fluorescence decays, while the powders had shorter multiexponential decays. Exposure of both types of samples to high laser fluence was also shown to induce faster excited state decay dynamics as observed using fluorescence and diffuse reflectance. In addition to the more rapid decays, these molecular crystals exhibited relatively high photobleaching quantum yields on the order of 10^{-4} . Previous work that interpreted picosecond decays in the transient absorption as evidence for rapid recombination and charge dissociation should be re-evaluated based on the susceptibility of this class of compounds to mechanical and photochemical damage.



INTRODUCTION

The existence of low energy charge transfer (CT) electronic states in donor–acceptor complexes makes these useful systems for studying how molecular interactions can affect electron–hole delocalization and transfer rates.¹ Molecular donor–acceptor cocrystals are chemically simple and structurally well-defined, making them ideal systems to study CT phenomena.² Technological applications may result from the ability to grow such crystals into different shapes, for example nanorods.³ McConnell et al. showed that all CT crystals could be grouped into two broad classes: ionic ground state CT, where the ground state involves an electron that has already been transferred, and nonionic ground state, where an electron transfer occurs only after absorption of a photon provides sufficient energy.⁴ Both types of CT crystals have been the subject of extensive research interest. Ionic CT crystals or CT salts can function as organic conductors and even superconductors. Nonionic CT crystals are neutral in their ground state, but undergo excited state photoinduced electron transfer reactions. Several groups have studied the time scale of charge separation in nonionic CT crystal systems, with the general conclusion that the CT state is populated within a few hundred femtoseconds after excitation of the neutral state.^{5–7} The separated charges recombine when they relax back to the ground state, providing a second opportunity to study electron transfer dynamics. The recombination of charge separated states in solution complexes has been extensively studied,^{8–11} but there is much less data on recombination in CT crystals. In this context, previous work by Kochi and

co-workers was especially intriguing.¹² Using transient absorption (TA) spectroscopy on powdered samples, they found that the CT excited state relaxation in a variety of tetracyanobenzene (TCNB)–donor complexes proceeded via two channels: recombination to the ground state and dissociation into free carriers. Both processes were complete within a few hundred picoseconds in the crystals studied. The yield of carrier dissociation was significant in all cases, and approached 50% for some crystals. This high yield of dissociated charges, coupled with reports of high photoconductivity in appropriately structured CT crystals,^{13,14} suggested to us that CT crystals might be able to function as highly ordered analogues of the bulk heterojunction structures commonly used to achieve high efficiency photovoltaics.¹⁵ It is possible to generate CT crystals with absorptions extending into the near-infrared, and thus these materials might constitute a molecular crystal alternative to polymer-based bulk heterojunction photovoltaic materials.

We have re-examined a subset of the TCNB compound originally studied in ref 12 in order to better understand the origins of the efficient charge dissociation. In all compounds, we found that the CT fluorescence survived for nanoseconds, much longer than the lifetimes derived from the earlier TA experiments. By doing careful power dependence measurements and comparing single crystal and powdered samples, we have determined that this

Received: November 15, 2010

Revised: January 13, 2011

Published: February 14, 2011

class of CT crystals is highly susceptible to both mechanical and photochemical damage. Both types of damage resulted in more rapid excited state relaxation dynamics as measured by both fluorescence and TA decays. We see no evidence of rapid dissociation of the CT electron–hole pair, and the dynamics appeared to be consistent with the traditional picture of a relatively tightly bound electron–hole pair that decays slowly back to the ground state. We do see a similar trend of recombination rate with charge transfer energy (E_{CT}) as seen in reference,¹² but with measured recombination rates that are now 1–2 orders of magnitude slower. Our work does not rule out the formation of other types of long-lived states such as triplets or dissociated charge carriers, but their formation rates must be relatively slow in order to be consistent with the nanosecond fluorescence lifetimes. These systems are thus quite different from the polymer bulk heterojunction systems, where dissociation into free carriers occurs on femtosecond to picosecond time scales.¹⁶

EXPERIMENTAL SECTION

Sample Preparation. CT single crystals were made by slow evaporation of concentrated 1:1 solutions of donor and acceptor in acetone in the dark at room temperature. Powder samples were prepared by combining a small quantity of single crystals with BaSO_4 powder (1–4 μm particle size, Alfa Aesar) and grinding them together for 25 min in an agate mortar and pestle. The resulting powders were 2% CT complex by weight. All crystals and powders were stored in the dark. Prior to measurements, crystal samples were affixed to glass substrates with a small quantity of nonfluorescent vacuum grease, typically applied to only one part of the crystal which was thereafter avoided when making measurements. For fluorescence experiments, powdered samples were sandwiched between two glass substrates, forming an optically thick layer. For diffuse reflectance TA experiments, about 100 mg of powder was put into a quartz cuvette that could be evacuated and backfilled with Argon gas to prevent oxygen contamination.

All chemicals were obtained commercially (Aldrich) and used as received. To test whether chemical impurities were affecting our spectroscopic results, naphthalene and TCNB were purified separately by sublimation and distillation, respectively. CT crystals grown from the purified components exhibited the same behavior as those grown using unpurified compounds.

Spectroscopy. The steady state fluorescence of the crystals and powders was measured in a Spex Fluorolog 3, using 400 nm excitation and front-face detection. Time-resolved fluorescence measurements were performed under vacuum in a Janis ST100 cryostat using a regeneratively amplified 40 kHz Spectra-Physics Ti:Sapphire laser system. The 800 nm output pulse was frequency doubled to 400 nm, and residual 800 nm light was removed using a dichroic mirror and two Schott glass BG39 filters. Various neutral density filters were used to ensure that the fluence per pulse was $2 \times 10^{-7} \text{ J/cm}^2$ or less for a typical scan. The sample fluorescence was collected from the front face of the sample and directed through a polarizer set at the magic angle (54.7°) angle relative to the pump beam polarizer. Two Schott glass OG420 color filters eliminated scattered light from the excitation laser beam. The fluorescence decays were measured with a Hamamatsu C4334 Streakscope. For the comparison of the fluorescence signals before and after laser exposure, the Streakscope signals were measured at low fluence on a fresh sample position, which was then subjected to a per-pulse fluence at

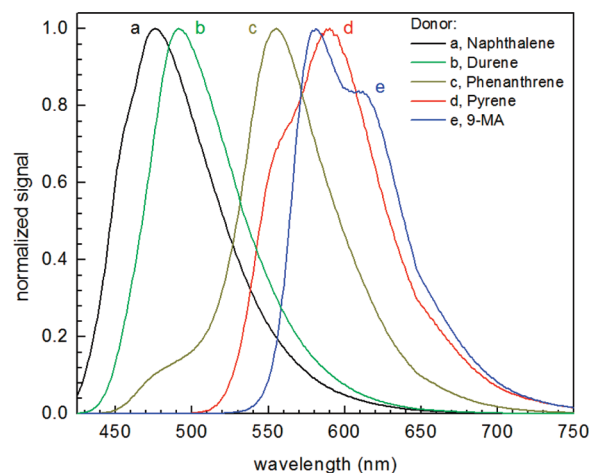


Figure 1. Normalized steady state fluorescence spectra of TCNB CT crystals. The excitation source was set to 400 nm for all compounds to match the laser excitation source used in the time-resolved fluorescence experiments.

400 nm of $5 \times 10^{-4} \text{ J/cm}^2$, for 60 s. The same spot was then measured again at low fluence. Fluorescence bleaching experiments were conducted in a similar fashion, but with the laser pulse fluence varying from $3.8 \times 10^{-6} \text{ J/cm}^2$ to $5.3 \times 10^{-4} \text{ J/cm}^2$ and using a 180 s exposure time.

Diffuse reflectance TA signals^{17–19} were measured using the same 40 kHz laser system. A portion of the 800 nm beam was diverted into a sapphire plate to generate a white continuum as the probe and the rest used to generate the 400 nm pump beam. The pump beam was chopped at 150 Hz and the modulated portion of the reflected probe beam was detected using a photodiode connected to a Stanford Research Systems Model SR830 DSP Lock-In Amplifier. Simultaneous detection with a probe reference channel was used to improve the signal-to-noise of the differential reflectance, $\Delta R/R$. The delay between the pump and probe pulses was varied using a 5 cm delay stage in the probe beam's path. The signal from the lock-in and the positioning of the delay stage were monitored and controlled by LabVIEW software.

RESULTS AND DISCUSSION

The steady-state emission spectra for the five CT molecular crystals studied in this work, along with the donor molecular structures, are shown in Figure 1. All the emission spectra have broad, featureless lineshapes. The phenanthrene crystal exhibited a pronounced shoulder at shorter wavelengths, indicating the presence of a second emitting state. The fluorescence spectra of powdered samples of these compounds were very similar to those of the single crystals shown in Figure 1. For all cases, the fluorescence could be easily observed in the solid state, in contrast to the analogous donor–acceptor complexes in solution, where the nonrigid environment permits rapid internal conversion and recombination to the ground state.²⁰

The strong steady-state fluorescence indicated a reasonably long fluorescence lifetime, and that is exactly what was observed for all five CT complexes in the solid state. For the single crystals, the fluorescence lifetimes extended well into the nanosecond regime, as shown in Figure 2 and in Table 1a. Note that the fluorescence decays plotted in Figures 2 and 3 are for data taken at the peak wavelength of the emission. For all compounds the fluorescence lifetime varied slightly with detection wavelength,

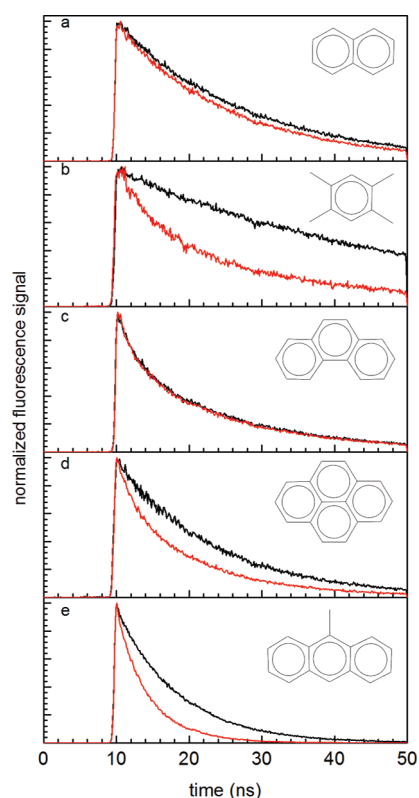


Figure 2. Normalized time-resolved fluorescence decays of TCNB CT crystals before and after (in red) a 60 s laser exposure of $500 \mu\text{J}/\text{cm}^2$. Donors: (a) naphthalene, (b) durene, (c) phenanthrene, (d) pyrene, (e) 9-MA.

and for this reason we report fluorescence decay times for two representative wavelengths in Table 1. In four of these compounds, this variation did not result in a qualitative change in spectral shape, leading us to conclude that the nature of the electronic state is the same, but due to heterogeneity in the crystal, different energy sites experience slightly different relaxation times. The exception was TCNB:phenanthrene, where we observed a clear multiexponential decay indicative of energy relaxation between two emissive states. This compound has an initially excited emission at 508 nm that decayed on a 1.7 ns time scale while the emission at 556 nm grew in on the same time scale and then persisted for tens of nanoseconds. Our measured fluorescence lifetimes are reasonably consistent with those reported earlier in the literature. TCNB:naphthalene crystals are the most extensively studied and have reported fluorescence lifetimes ranging from 17 to 21 ns,^{21–23} which is exactly the range we measure depending on the detection wavelength. TCNB:durene has a reported lifetime of 34 ns,²⁴ as compared to 46–48 ns in Table 1a. The largest discrepancy is for TCNB:pyrene, where the fluorescence lifetime has been reported as 31.5 ns,²² considerably longer than the 14–16 ns reported in Table 1. The variation in fluorescence lifetimes for these CT crystals may reflect their sensitivity to preparation conditions, as discussed below. All the decays summarized in Table 1 were measured using a very low laser fluence of $2 \times 10^{-7} \text{ J}/\text{cm}^2$ per pulse or less. After exposure to higher fluences, we noticed that the fluorescence signals decreased, and the decays became more rapid, especially for the durene, pyrene and 9-methylantracene (9-MA) crystals. The normalized

Table 1

| (a) Fluorescence Lifetimes of TCNB CT Single Crystals | | | | | |
|---|----------------------------|----------------|----------------|-------|-------|
| donor | λ_{fl} (nm) | τ_1 (ns) | τ_2 (ns) | a_1 | a_2 |
| naphthalene | 476 | 17.3 ± 0.5 | | 1 | |
| | 555 | 21.1 ± 0.5 | | 1 | |
| durene | 492 | 48.1 ± 0.5 | | 1 | |
| | 570 | 46.5 ± 0.5 | | 1 | |
| phenanthrene | 508 | 1.7 ± 0.2 | 14.8 ± 0.5 | 0.38 | 0.62 |
| | 556 | 1.8 ± 0.2 | 34.5 ± 0.5 | −0.72 | 1.72 |
| pyrene | 590 | 13.6 ± 0.5 | | 1 | |
| | 640 | 15.5 ± 0.5 | | 1 | |
| 9-MA | 582 | 8.3 ± 0.2 | | 1 | |
| | 674 | 7.8 ± 0.3 | | 1 | |

| (b) Fluorescence Lifetimes of TCNB CT Powders in BaSO_4 | | | | | |
|--|----------------------------|----------------|----------------|-------|-------|
| donor | λ_{fl} (nm) | τ_1 (ns) | τ_2 (ns) | a_1 | a_2 |
| naphthalene | 459 | 14.1 ± 0.3 | | 1 | |
| | 591 | 34 ± 1 | | 1 | |
| durene | 480 | 2.0 ± 0.2 | 18.7 ± 0.3 | 0.149 | 0.85 |
| | 582 | 25.4 ± 0.3 | | 1 | |
| phenanthrene | 473 | 1.5 ± 0.1 | 9.4 ± 0.1 | 0.67 | 0.33 |
| | 550 | 1.2 ± 0.2 | 30.3 ± 0.2 | −0.51 | 1.51 |
| pyrene | 564 | 1.5 ± 0.1 | 13.4 ± 0.3 | 0.29 | 0.71 |
| | 664 | 19.5 ± 0.1 | | 1 | |
| 9-MA | 595 | 0.6 ± 0.1 | 4.1 ± 0.3 | 0.527 | 0.473 |
| | 681 | 0.6 ± 0.1 | 4.5 ± 0.3 | 0.23 | 0.770 |

fluorescence decays after a total laser dose of $1200 \text{ J}/\text{cm}^2$ (i.e., $5 \times 10^{-4} \text{ J}/\text{cm}^2$ per pulse at 40 kHz over a 60 s period) exhibited a significant increase in the fluorescence decay rates, and these damage-induced decays are overlaid with the original signals in Figure 2. The change in lifetime depended on the compound: TCNB:naphthalene's decay was only about 15% faster, while for durene and 9-MA the decay was almost twice as rapid in the photodamaged crystal as compared to the pristine single crystal. The fluorescence decays of the powdered samples before and after laser exposure are shown in Figure 3, while the decay parameters at different wavelengths are summarized in Table 1b. The same photoinduced acceleration of the fluorescence decay was observed for the powdered samples, with the main difference being that the initial decay rates were now much faster than in the single crystals, presumably as a result of damage during the mechanical grinding process. Note that the powder decays tended to be more rapid and possessed a pronounced biexponential character at most wavelengths. The susceptibility of the TCNB CT crystals to photo-damage was much more pronounced than in other molecular crystal systems that we have studied. For example, a perylene single crystal exposed to the same laser dose showed no measurable photobleaching or change in fluorescence decay rate.

Clearly, the CT crystals are vulnerable to damage, both via mechanical milling and via prolonged exposure to light. These two types of damage appear to act through different mechanisms. For example, mechanical grinding had a large effect on the decay of TCNB:phenanthrene, but this solid was largely unaffected by laser exposure, as seen by comparing the fluorescence decays in Figures 2c and 3c. Quantifying the amount of damage as a function of mechanical stress is difficult due to the uncontrolled nature of the grinding process. Quantifying the amount of

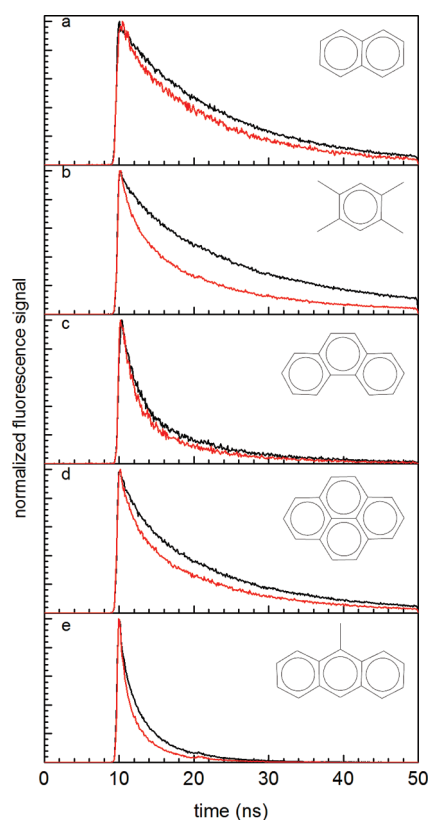


Figure 3. Normalized time-resolved fluorescence decays of dilute pulverized TCNB CT crystals in BaSO_4 powder before and after (in red) a 60 s laser exposure of $500 \mu\text{J}/\text{cm}^2$. Donors: (a) naphthalene, (b) durene, (c) phenanthrene, (d) pyrene, (e) 9-MA.

photodamage is more straightforward since one can precisely control the laser exposure. There are different aspects of laser damage: changes in fluorescence lifetime and changes in the total amount of fluorescence signal. We first examined the decrease in total fluorescence signal, or photobleaching. Following the treatment of Kao et al.,²⁵ we find that the fluorescence signal P decays after N pulses according to

$$P(N) = P(0) \exp \left[-\beta \left(\frac{F}{h\nu} \right)^M N \right] \quad (1)$$

where $h\nu$ is the pulse energy, F is the pulse energy per unit area, and β is the bleaching cross section. From eq 1 we see that a plot of $\ln[-\ln(P(N)/P(0))]$ versus $\ln(F)$ should yield a straight line with slope M giving the multiphoton power law. In Figure 4, a log–log plot of the bleach fraction versus the accumulated fluence for TCNB:9-MA yielded a slope $M = 0.99 \pm 0.09$, indicating that the photobleaching proceeds through a single photon process with $M = 1$. For TCNB:naphthalene, we could also extract $\beta = 4.1 \times 10^{-22} \text{ cm}^2$ from this plot. The ratio of β to the absorption cross section σ_{abs} gives the photobleaching yield Φ_{bleach} ²⁵

$$\Phi_{\text{bleach}} = \frac{\beta}{\sigma_{\text{abs}}} \quad (2)$$

Using eq 2 and the value $\sigma_{\text{abs}} = 9.2 \times 10^{-18} \text{ cm}^2$ for the absorption cross section at 400 nm,²¹ we find $\Phi_{\text{bleach}} = 4.4 \times 10^{-5}$ for this CT crystal in powder form. We observed similar single

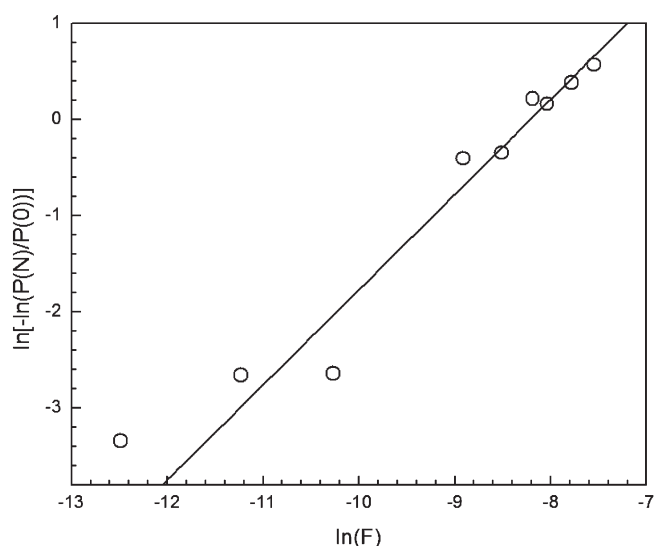


Figure 4. Log–log plot of normalized fluorescence signal, $P(N)/P(0)$, versus laser fluence, F , for TCNB:9-MA in BaSO_4 powder. Each data point is the result from a fresh spot on the sample, where its total integrated fluorescence signal was measured twice, before and after photodamage at a fixed fluence and time duration. Using these results in eq 1, the calculated slope was 0.99 ± 0.09 , indicating that the photobleaching of the sample occurred via a single photon process.

photon bleaching behavior for the four other compounds in this study, all with Φ_{bleach} values of approximately 10^{-4} to 10^{-5} . Typical organic dyes have $\Phi_{\text{bleach}} = 10^{-6}$ or less in solution,^{25,26} so this value is surprisingly high for a polycrystalline sample under vacuum. We also observed that while the integrated fluorescence signal was bleaching, the fluorescence decay rate was also becoming more rapid. The biexponential decays are fit to the function $a_1 \exp[t/\tau_1] + a_2 \exp[t/\tau_2]$ and Figure 5a shows the change in the average fluorescence decay time τ_{avg} for TCNB:9-MA powder, defined as

$$\tau_{\text{avg}} = \frac{a_1 \tau_1 + a_2 \tau_2}{a_1 + a_2} \quad (3)$$

For comparison, the decrease in the total fluorescence signal, $P(N)/P(0)$ is shown in Figure 5b for this compound. From Figure 5, it can be seen that the decrease in fluorescence decay time and the decrease in total fluorescence signal parallel each other. It is important to note, however, that τ_{avg} decreased only $\sim 20\%$, while the total fluorescence decreased by $\sim 80\%$. The large decrease in total fluorescence signal thus cannot be due solely to the observed decrease in τ_{avg} . However, the data in Figure 5 strongly suggest that both changes are manifestations of the same damage process.

At even higher laser fluence levels, we have found that the TCNB:naphthalene TA kinetics can be affected by photodamage as well. Figure 6 shows the pump–probe kinetics for a 400 nm excitation pulse followed by a 700 nm probe pulse. Seven hundred nanometers is close to the peak of the naphthalene radical cation absorption, and this spectral region was also monitored in ref 12 to measure the disappearance of the CT species due to recombination. Due to the low absorption coefficients of these compounds (typically $\sim 1000 \text{ M}^{-1} \text{ cm}^{-1}$ or less), relatively high pump pulse fluences were required to obtain reasonable pump–probe signal levels. At a pump pulse fluence of $2.6 \times 10^{-4} \text{ J}/\text{cm}^2$,

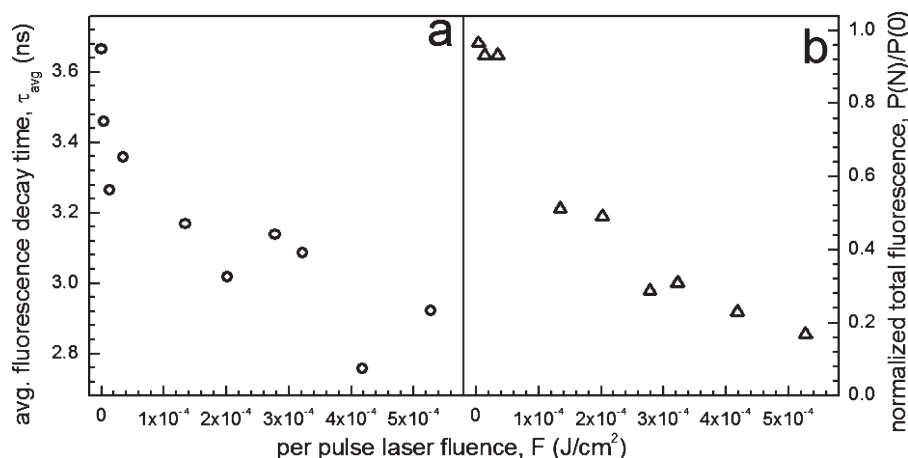


Figure 5. (a) Average fluorescence decay time, τ_{avg} defined by eq 3, and (b) normalized total fluorescence signal, $P(N)/P(0)$ versus the per pulse laser fluence for TCNB:9-MA. The total exposure to this per pulse fluence was, at a repetition rate of 40 kHz, for 180 s. The shortening of the decay time and the fluorescence signal bleaching exhibit a similar dependence on the pulse fluence F .

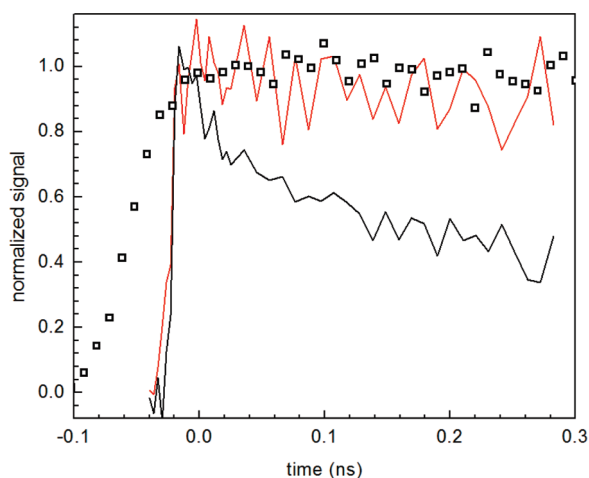


Figure 6. Normalized time-resolved fluorescence signal (\square) and TA ($\Delta R/R$) for an unexposed sample (red) and after exposure to a total fluence of 1.4×10^5 J/cm² (black) of TCNB:naphthalene in BaSO₄ powder. Like the fluorescence, TA measurements of a fresh sample exhibited only a slow decay. Note that the lowest feasible fluence for the TA experiments was 2.6×10^{-4} J/cm², whereas the fluorescence measurements were done at a laser pulse fluence of 2×10^{-7} J/cm² or lower.

the highest fluence where no obvious damage occurs during a scan of the pump–probe delay, the peak $\Delta R/R$ signal was on the order of 2.7×10^{-4} . This signal was a factor of 1000 lower than that detected in ref 12. Figure 6 shows that at this fluence level, the 700 nm induced absorption appeared within the time resolution of the experiment (200 fs) and showed no decay over the next 300 ps. This signal is overlaid with the fluorescence decay obtained from the streak camera measurements in Figure 6. When the pump pulse fluence was increased to 9.4×10^{-4} J/cm², where the $\Delta R/R$ signal level was on the order of 10^{-3} , the signal developed a second decay component on the order of 100 ps. This more rapid decay persisted even when the experiment was repeated on the same sample spot with lower pump power. Shown in Figure 6 is the TA decay measured using the pump pulse fluence of 2.6×10^{-4} J/cm² after the sample had been subjected to a total fluence of 1.4×10^5 J/cm² over the period of

~1 h. This dose was considerably higher than what was used in the fluorescence photodamage experiments, and now the damage-induced decay has moved into the subnanosecond range. The lifetime obtained from the TA decay in Figure 5 was 120 ps, about a factor of 2 shorter than that observed in ref 12 for the same compound. This difference may be due to a difference in laser exposure conditions, but since parameters such as laser spot size and pulse energy were not reported in ref 12, we cannot be certain that this is the case. We also have not surveyed other TCNB complexes to see whether they exhibit the same trend of damage-induced decays in their TA spectra, although, since they all showed similar sensitivities in their fluorescence decays, it is likely that photodamage can affect their TA response dynamics as well.

Our results indicate that the TCNB CT solids are highly susceptible to damage, both due to mechanical and photochemical processes. This may be a byproduct of the bicomponent nature of the crystals, since it may be easier to produce defects when one component can be displaced from the lattice due to heating or a chemical reaction. In some sense, the CT crystal is only as strong as its weakest link, which in this case is probably the low molecular weight TCNB. One measure of the weak TCNB-donor packing forces is the significant orientational disorder in TCNB:naphthalene crystals at room temperature, as measured by both X-ray diffraction²⁷ and by Raman spectroscopy.²⁸ Similar disorder has also been observed in other TCNB:donor molecular crystals.^{29,30} Presumably, this orientational disorder could also create sites with different energies and decay times, which would help explain the wavelength-dependent decays of the fluorescence spectra. For higher molecular weight acceptors, such as tetracyanoquinodimethane (TCNQ), it is possible that the lattice would be more resistant to disruption. Preliminary studies in our group on both the photoluminescence and TA of TCNQ:pyrene have shown this compound to be less sensitive to grinding and laser exposure than TCNB:pyrene. A second possible origin of the damage susceptibility of these crystals is the nature of the CT excited state itself, which may be more prone to side reactions than a neutral excited state.

Given the sensitivity of the TCNB CT complexes to preparation conditions such as grinding, as well as to experimental conditions such as laser exposure, it becomes a difficult question as to how to determine the true charge recombination time. The

analysis of this recombination time in terms of electron transfer theory was the main result of ref 12. Clearly, the most straightforward systems to analyze are the pristine single crystals under low laser irradiance. As shown in Table 1, four of the five compounds exhibited a single exponential decay at all wavelengths, on the order of 10 ns or longer. TCNB:phenanthrene appears to have an initial state that relaxes to the longer-lived CT state within a few nanoseconds. The ultimate charge recombination back to the ground state is likely reflected by the longest fluorescence lifetime in the single crystals. If we neglect intersystem crossing and charge dissociation into free carriers, we are left with only the internal conversion and radiative recombination mechanisms. In ref 12 it was assumed that the nonradiative electron transfer pathway was dominant. Given the much longer excited state lifetimes deduced in the current work, the neglect of the radiative pathway may no longer be justified. Nevertheless, if we follow ref 12 and assume that the recombination electron transfer rate k_{recomb} depends on the energy difference E_{CT} between the CT and neutral state, we find a similar trend as in the earlier work, albeit for a smaller set of compounds. Of course, our recombination rates are a factor of 100 smaller than those reported in ref 12. Given that our decay rates only vary by a factor of 6 for this set of compounds, it would be premature to try to extract any definite relation between the recombination rate and E_{CT} . To do this would require a survey of a larger number of donor molecules. We simply point out that our limited data do not contradict the electron transfer theory used in ref 12 to analyze its results.

CONCLUSION

Our results on CT crystals of various donors complexed with TCNB indicate that caution must be used when studying their photophysical properties. First, these solids can have multiple excited states and complicated, multiexponential decay dynamics. Second, both mechanical stress and light exposure can cause various relaxation processes to become more rapid, as well as reducing signal intensity through a high yield photobleaching process. In general, the kinetic parameters of a TCNB CT molecular crystal sample will depend on its preparation conditions and laser exposure history, and its sensitivity to these parameters will depend on its molecular composition. The samples that provided the simplest decay dynamics and consistent results were pristine single crystals, and it is recommended that results obtained on powdered samples be compared to single crystal results whenever possible. To measure TA data, it may be that liquid suspensions of nanocrystals^{31,32} are superior to stationary powders in order to prevent damage effects. From the standpoint of the photodynamics of these compounds, our results are consistent with the picture of long-lived, Coulombically bound states that undergo relatively slow charge recombination. The one compound that did exhibit a relatively rapid (1.8 ns) fluorescence decay clearly involved relaxation to a lower energy emissive state and not charge dissociation into free carriers. We find no evidence for the rapid dissociation channel inferred by Kochi and co-workers in ref 12 and ascribe the picoseconds dynamics observed in that work to unintentional photodamage. This class of CT crystals may provide a good testbed for theories of electron transfer and bound CT states, but probably is not a good analogue for bulk heterojunction systems where full charge separation takes place with close to 100% efficiency.

AUTHOR INFORMATION

Corresponding Author

*E-mail: christopher.bardeen@ucr.edu.

ACKNOWLEDGMENT

This research was supported by the Department of Energy, Basic Energy Sciences, Grant DOE-FG02-09ER16096.

REFERENCES

- (1) Kochi, J. K. Charge-transfer excitation of molecular complexes in organic and organometallic chemistry. *Pure Appl. Chem.* **1991**, *63*, 255–264.
- (2) Wright, J. D., *Molecular Crystals*, 2nd ed.; Cambridge University Press: Cambridge, U.K., 1995.
- (3) Al-Kaysi, R. O.; Muller, A. M.; Frisbee, R. J.; Bardeen, C. J. Formation of cocrystal nanorods by solid-state reaction of tetracyanobenzene in 9-methylantracene molecular crystal nanorods. *Cryst. Growth Des.* **2009**, *9*, 1780–1785.
- (4) McConnell, H. H.; Hoffman, B. M.; Metzger, R. M. Charge transfer in molecular crystals. *Proc. Nat. Acad. Sci. U.S.A.* **1965**, *53*, 46–50.
- (5) Fukazawa, N.; Fukamura, H.; Masuhara, H.; Prochorow, J. A picosecond diffuse reflectance laser photolysis study on phenanthrene–pyromellitic dianhydride charge-transfer crystal. *Chem. Phys. Lett.* **1994**, *220*, 461–466.
- (6) Asahi, T.; Matsuo, Y.; Masuhara, H. Localization of a charge transfer excited state in molecular crystals: A direct confirmation by femtosecond diffuse reflectance spectroscopy. *Chem. Phys. Lett.* **1996**, *256*, 525–530.
- (7) Asahi, T.; Matsuo, Y.; Masuhara, H.; Koshima, H. Electronic structure and dynamics of the excited state in CT microcrystals as revealed by femtosecond diffuse reflectance spectroscopy. *J. Phys. Chem. A* **1997**, *101*, 612–616.
- (8) Ojima, S.; Miyasaka, H.; Mataga, N. Femtosecond–picosecond laser photolysis studies on the dynamics of excited charge-transfer complexes in solution. 3. Dissociation into free ions and charge recombination decay from the ion pair state formed by charge separation in the excited state of 1,2,4,5-tetracyanobenzene hydrocarbon complexes in polar solvents. *J. Phys. Chem.* **1990**, *94*, 7534–7539.
- (9) Hubig, S. M.; Bockman, T. M.; Kochi, J. K. Optimized electron transfer in charge-transfer ion pairs. Pronounced inner-sphere behavior of olefin donors. *J. Am. Chem. Soc.* **1996**, *118*, 3842–3851.
- (10) Nicolet, O.; Vauthey, E. Ultrafast nonequilibrium charge recombination dynamics of excited donor–acceptor complexes. *J. Phys. Chem. A* **2002**, *106*, 5553–5562.
- (11) Mohammed, O. F.; Vauthey, E. Simultaneous generation of different types of ion pairs upon charge-transfer excitation of a donor–acceptor complex revealed by ultrafast transient absorption spectroscopy. *J. Phys. Chem. A* **2008**, *112*, 5804–5809.
- (12) Hubig, S. M.; Kochi, J. K. Photoinduced electron transfer in charge-transfer crystals by diffuse reflectance (picosecond) time-resolved spectroscopy. *J. Phys. Chem.* **1995**, *99*, 17578–17585.
- (13) Vincent, V. M.; Wright, J. D. Photoconductivity and crystal structure of organic molecular complexes. *J. Chem. Soc., Faraday Trans. 1* **1974**, *70*, 58–71.
- (14) Samoc, M.; Williams, D. F. Photoconductivity in crystals of charge-transfer complex anthracene–tetracyanobenzene. *J. Chem. Phys.* **1983**, *78*, 1924–1930.
- (15) Gunes, S.; Neugebauer, H.; Sariciftci, N. S. Conjugated polymer-based organic solar cells. *Chem. Rev.* **2007**, *107*, 1324–1338.
- (16) Hwang, I. W.; Moses, D.; Heeger, A. J. Photoinduced carrier generation in P3HT/PCBM bulk heterojunction materials. *J. Phys. Chem. C* **2008**, *112*, 4350–4354.
- (17) Colombo, D. P.; Bowman, R. M. Does interfacial charge transfer compete with charge carrier recombination? A femtosecond diffuse reflectance investigation of TiO₂ nanoparticles. *J. Phys. Chem.* **1996**, *100*, 18445–18449.

- (18) Asahi, T.; Furube, A.; Fukumura, H.; Ichikawa, M.; Masuhara, H. Development of a femtosecond diffuse reflectance spectroscopic system, evaluation of its temporal resolution, and applications to organic powder systems. *Rev. Sci. Instrum.* **1998**, *69*, 361–371.
- (19) Kamat, P. V.; Gevaert, M.; Vinodgopal, K. Photochemistry on semiconductor surfaces. Visible light induced oxidation of C₆₀ on TiO₂ nanoparticles. *J. Phys. Chem. B* **1997**, *101*, 4422–4427.
- (20) Hinatu, J.; Yoshida, F.; Masuhara, H.; Mataga, N. On the relationship between ionic photodissociation yield and electron donor–acceptor interaction of 1,2,4,5-tetracyanobenzene and pyromellitic dianhydride complexes. *Chem. Phys. Lett.* **1978**, *59*, 8083.
- (21) Yoshihara, K.; Inoue, A.; Nagakura, S. Effect of high density excitons on fluorescence of naphthalene–tetracyanobenzene complex crystal. *Chem. Phys. Lett.* **1972**, *13*, 459–462.
- (22) Kozmenko, M. V.; Kuzmin, M. G. Luminescence of crystalline complexes of tetracyanobenzene with aromatic hydrocarbons. *Zh. Prikl. Spektrosk.* **1977**, *27*, 429–434.
- (23) Betz, E.; Port, H.; Schrof, W.; Wolf, H. C. Energy transfer and exciton self-trapping in the charge-transfer crystal naphthalene–tetracyanobenzene. *Chem. Phys.* **1988**, *128*, 73–81.
- (24) Kobayashi, T.; Nagakura, S. The biexcitonic quenching and excitation migration rate in aromatic crystals. *Mol. Phys.* **1972**, *24*, 695–704.
- (25) Kao, F. J.; Wang, Y. M.; Chen, J. C.; Cheng, P. C.; Chen, R. W.; Lin, B. L. Photobleaching under single photon and multi-photon excitation: Chloroplasts in protoplasts from *Arabidopsis thaliana*. *Opt. Commun.* **2002**, *201*, 85–91.
- (26) Eggeling, C.; Widengren, J.; Rigler, R.; Seidel, C. A. M. Photobleaching of fluorescent dyes under conditions used for single molecule detection: Evidence for two step photolysis. *Anal. Chem.* **1998**, *70*, 2651–2659.
- (27) Kumakura, S.; Iwasaki, F.; Saito, Y. The crystal structure of the 1:1 complex of naphthalene with 1,2,4,5-tetracyanobenzene. *Bull. Chem. Soc. Jpn.* **1967**, *40*, 1826–1833.
- (28) Macfarlane, R. M.; Ushioda, S. Raman study of orientational disorder in the molecular charge-transfer crystals naphthalene-TCNB and naphthalene-PMDA. *J. Chem. Phys.* **1977**, *67*, 3214–3220.
- (29) Boeyens, J. C. A.; Levendis, D. C. Static disorder in crystals of anthracene–tetracyanobenzene charge transfer complex. *J. Chem. Phys.* **1984**, *80*, 2681–2688.
- (30) Muhle, W.; Krzystek, J.; Schutz, J. U. V.; Wolf, H. C.; Stigler, R. D.; Stezowski, J. J. The 1:1 charge-transfer crystal fluorene-1,2,4,5-tetracyanobenzene (F-TCNB): Triplet excitons, optical and structural properties. *Chem. Phys.* **1986**, *108*, 1–13.
- (31) Chin, K. K.; Natarajan, A.; Gard, M. N.; Campos, L. M.; Shepherd, H.; Johansson, E.; Garcia-Garibay, M. A. Pump–probe spectroscopy and circular dichroism of nanocrystalline benzophenone – Towards absolute kinetic measurements in solid state photochemical reactions. *Chem. Commun.* **2007**, 4266–4268.
- (32) Kuzmanich, G.; Gard, M. N.; Garcia-Garibay, M. A. Photonic amplification by a singlet-state quantum chain reaction in the photodecarbonylation of crystalline diarylcyclopropanone. *J. Am. Chem. Soc.* **2009**, *131*, 11606–11614.